A Compensation Method for Magnetic Localization on Capsule Robot in Medical Application

Qiang Fu, Chunliu Fan, Xinrui Wang, Songyuan Zhang, Xi Zhang, Jian Guo, and Shuxiang Guo, *Fellow, IEEE*

***Abstract*—Aiming at the magnetic positioning accuracy of capsule robot and the magnetic coupling between capsule robot and external driving magnetic field, according to the requirements of capsule robot for position and attitude information, a magnetic positioning compensation method of capsule robot based on magnetic driving system is proposed. This method deduces the error formula according to the magnetic dipole model, optimizes the formula, reduces the number of unknowns, optimizes the calculation process and improves the positioning accuracy. At the same time, a compensation is added to solve the magnetic coupling problem between the external driving magnetic field three-axis Helmholtz coil and the capsule robot. Finally, several groups of experiments verify the effectiveness of the algorithm.**

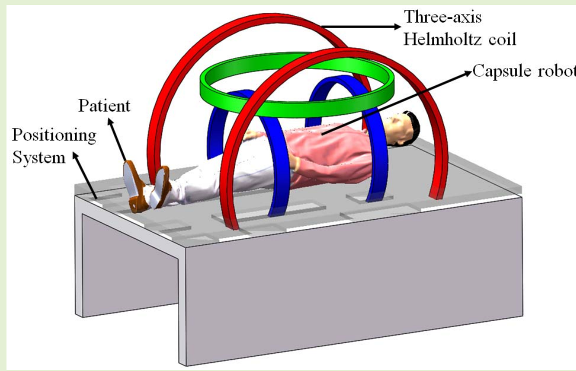

***Index Terms*— Capsule robot, compensation algorithm, magnetic localization.**

I. Introduction

NOWADAYS, with the continuous progress of science and technology, compared with the traditional electronic endoscope, painless and noninvasive capsule robot detection has become the first choice for gastrointestinal examination [1]–[3]. When the capsule robot is used for gastrointestinal examination, doctors need to quickly find the location of lesions for diagnosis and treatment through the accurate positioning of the capsule robot in the human body [4]–[6]. At present, magnetic positioning technology has been widely used in the positioning of capsule robots. Magnetic positioning can improve the positioning accuracy of the robot and is conducive to medical diagnosis and treatment. In this technology, the magnetic induction intensity of the permanent magnet in the capsule robot is measured by the magnetic sensor to determine the position of the capsule robot in real-time [7]–[10]. However, the positioning of the capsule robot will be affected by gastrointestinal peristalsis and external driving equipment. Therefore, how to realize the accurate positioning of capsule robots in the human gastrointestinal tract has become a research topic. In order to solve this problem, many researchers have done much research on the magnetic positioning model and algorithm of capsule robots [11]–[14]. Liao Ying *et al.* proposed an external magnetic field positioning system based on Hall effect sensors array [15]. The system uses a sensor array to measure the magnetic induction intensity of permanent magnet and then uses the Levinberg-Maguilt algorithm to calculate the motion position and direction of capsule robot in vivo. The experimental results show that the positioning accuracy of this method is millimeter scale, which can meet the needs of practical application. Hu *et al.* proposed a compensation method for magnetic localization on the capsule endoscope

Manuscript received October 5, 2021; revised October 18, 2021; accepted October 18, 2021. Date of publication October 21, 2021; date of current version November 30, 2021. This work was supported in part by the Natural Science Foundation of Tianjin under Grant 18JCYBJC43200, in part by the Tianjin Key Laboratory for Control Theory and Application in Complicated Systems under Grant TJKL-CTACS-201903, and in part by the Innovative Cooperation Project of Tianjin Scientific and Technological Support under Grant 18PTZWHZ00090. The associate editor coordinating the review of this article and approving it for publication was Prof. Guiyun Tian. *(Corresponding author: Songyuan Zhang.)*

Qiang Fu and Jian Guo are with the Tianjin Key Laboratory for Control Theory and Application in Complicated Systems, Tianjin International Joint Research and Development Center, Tianjin University of Technology, Tianjin 300380, China (e-mail: fuqiang6369@hotmail.com; gj15102231710@163.com).

Chunliu Fan, Xinrui Wang, and Xi Zhang are with the Intelligent Robot Laboratory, Tianjin University of Technology, Tianjin 300380, China (e-mail: 2536723678@qq.com; 1175708424@qq.com; 549244209@qq.com).

Songyuan Zhang is with the State Key Laboratory of Robotics and System, Harbin Institute of Technology, Harbin 150001, China (e-mail: zhangsy@hit.edu.cn).

Shuxiang Guo is with the Department of Intelligent Mechanical Systems Engineering, Kagawa University, Takamatsu 761-0396, Japan (e-mail: guo@eng.kagawa-u.ac.jp).

Digital Object Identifier 10.1109/JSEN.2021.3121908

about the interference of body movement [16]. Two mutually perpendicular magnets are fixed as the reference target on the human body surface in this method. A specific algorithm compensates for the interference caused by the human body movement to reduce the interference of the human body to the final positioning result of the capsule robot. However, in the complex human environment, the positioning effect of the capsule robot is not ideal. Wang Min *et al.* proposed an algorithm combining absolute positioning and relative positioning [17]. The established sensor array measures the absolute position of the capsule robot, and then the Bessel curve fitting method is used. By calculating the actual movement distance caused by gastrointestinal peristalsis, the positioning of the capsule robot in a complex human environment is realized. Aiming at the problem of positioning accuracy, Ren Yupeng proposed a wireless capsule endoscope positioning technology based on a magnetic sensor array [18]. This technology is based on the analysis of the magnetic field distribution of the magnet, aiming at the problem that the magnetic dipole near field generation is not applicable, to propose a modified model to improve the accuracy. Niu proposed a capsule endoscope positioning technology based on magnetic induction [19], The positioning technology is based on the new multi magnetic dipole model and the particle filter magnetic positioning algorithm. It overcomes the problems of low model accuracy and small positioning range. However, the above studies do not consider the influence of magnetic coupling on the magnetic positioning accuracy of capsule robot, and the positioning accuracy needs to be improved. Our team's previous research on various driving systems, structures and motion characteristics of capsule robots, proposes a magnetic positioning compensation algorithm for capsule robots [20]–[22]. The compensation algorithm deduces the error fitting formula by establishing the magnetic dipole model and uses the least square method to fit the error of the actual position of the capsule robot in the human body. A new compensation position is obtained through the digital operation of the initial position to make it closer to the expected value. The algorithm solves the magnetic coupling problem and reduces the six variables in the original magnetic dipole model formula to three. In order to improve the positioning accuracy of the decoupled capsule robot, compensation is added to the magnetic positioning algorithm. The experimental results show that the algorithm effectively solves the magnetic coupling problem between the capsule robot and the external driving magnetic field, and improves the positioning accuracy of the robot.

II. Magnetic Localization Algorithm

A. Magnetic Dipole Model

The magnetic dipole model is a physical model established by analogy with the electric dipole model. Because the magnet in the capsule robot is tiny relative to the positioning system, that is, the radius of the permanent magnet in the capsule robot is much smaller than the distance from the sensor array to the permanent magnet so that the permanent magnet can be regarded as a magnetic dipole [23], and its mathematical model is shown in Fig. 1.

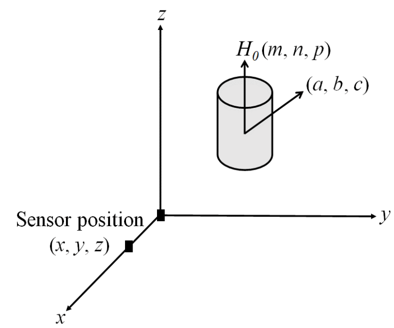

Fig. 1. Magnetic dipole model.

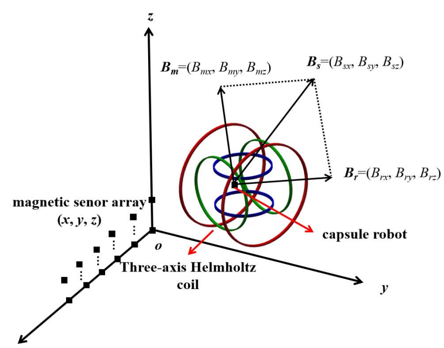

Fig. 2. Schematic diagram of capsule robot localization.

As shown in the coordinate system of Fig. 1, (a, b, c) represents the center of the permanent magnet, and (x, y, z) represents the coordinates of the sensor. $\boldsymbol{H_0} = (\boldsymbol{n}, \boldsymbol{p}, \boldsymbol{q})$ is the vector of the magnetic field direction of the permanent magnet, and $n^2 + p^2 + q^2 = 1$. Based on this model, the magnetic induction intensity of the permanent magnet measured by the sensor is $\boldsymbol{B} = (B_x, B_y, B_z)$, as shown in equation (1), as shown at the bottom of the page.

According to equation (1), six unknowns need to be solved in the whole positioning process, and the solution process is complex.

B. Compensation Method of Magnetic Positioning

A three-axis Helmholtz coil drives the motion of the capsule robot. The simplified model of the magnetic positioning system is shown in Fig 2 [24]. $\boldsymbol{B_s} = (B_{sx}, B_{sy}, B_{sz})$ is the magnetic field strength measured by the sensor, $\boldsymbol{B_m} = (B_{mx}, B_{my}, B_{mz})$ is the magnetic field strength of the energized

$$\begin{bmatrix} B_x \\ B_y \\ B_z \end{bmatrix} = \frac{\mu_0}{4\pi \mathrm{r}^5} \begin{bmatrix} 3[\mathrm{n}(x-a)+p(y-b)+q(z-c)](x-a)-nr^2 \\ 3[n(x-a)+p(y-b)+q(z-c)](y-b)-pr^2 \\ 3[n(x-a)+q(y-b)+q(z-c)](z-c)-qr^2 \end{bmatrix} \tag{1}$$

triaxial Helmholtz coil, and $\boldsymbol{B}_{\mathbf{r}} = (B_{rx},\ B_{ry},\ B_{rz})$ is the magnetic field strength of the embedded permanent magnet in the capsule robot. The relationship between the three is shown in equation (2):

$$\boldsymbol{B_s} = \boldsymbol{B_r} + \boldsymbol{B_m} \tag{2}$$

In this paper, the magnetic positioning system is applied 6×6. The magnetic induction intensity is measured on the sensor array platform, and the average values of $\boldsymbol{B}_{\mathbf{s}}$ is obtained from equation (3):

$$B_{\mathrm{s}} = \sum_{i=1}^{6}\sum_{j=1}^{6}\frac{\boldsymbol{B}_{sij}}{36} \tag{3}$$

On this basis, in order to decouple the magnetic coupling between the driving magnetic field and the permanent magnet in the capsule robot, an improved algorithm is proposed, as shown in equation (4):

$$\begin{aligned} B_{sx}-B_{mx} &= \frac{\mu_0}{4\pi}\{\frac{3[n(x-a)+p(y-b)+q(z-c)](x-a)}{r^5} - \frac{n}{r^3}\} \\ B_{sy}-B_{my} &= \frac{\mu_0}{4\pi}\{\frac{3[n(x-a)+p(y-b)+q(z-c)](y-b)}{r^5} - \frac{p}{r^3}\} \\ B_{sz}-B_{mz} &= \frac{\mu_0}{4\pi}\{\frac{3[n(x-a)+p(y-b)+q(z-c)](z-c)}{r^5} - \frac{q}{r^3}\} \end{aligned} \tag{4}$$

The direction of the magnetic dipole moment of the capsule robot driven by a three-axis Helmholtz coil is known. Assuming that the capsule robot moves along the positive direction of the z-axis of the sensor, the magnetic dipole moment of the capsule robot is (0,0, m). Equation (5) can be derived [25].

$$\frac{\mu_0}{4\pi r^5}\begin{bmatrix} 3zx \\ 3zy \\ 3z^2 - r^2 \end{bmatrix} - \begin{bmatrix} B_x - B_{mx} \\ B_y - B_{my} \\ B_z - B_{mz} \end{bmatrix} = 0 \tag{5}$$

When the Angle θ between the vector r and the positive direction of the Z axis is 0, equation (6) can be derived from equation (5).

$$\frac{|\mu|}{r^3}\begin{bmatrix} 3cos^2\theta - 1 \\ |3sin\theta cos\theta| \end{bmatrix} - \begin{bmatrix} \frac{B_{\mathrm{s}z} - B_{mz}}{\sqrt{(B_{sx}-B_{mx})^2 + (B_{sy}-B_{my})^2}} \end{bmatrix} = 0 \tag{6}$$

where:

$$|\mu| = \frac{\mu_0 m}{4\pi}$$

By substituting $cos2\theta$ and $sin2\theta$ into equation (6), we can get equation (7), as shown at the bottom of the page.

The relationship between magnetic sensor position and magnetic flux density is shown in equation (8).

$$\begin{bmatrix} x \\ y \\ z \end{bmatrix} = \frac{|10^{-7}m|^{\frac{1}{3}}t^{\frac{4}{3}}}{\sqrt{3}}\begin{bmatrix} \frac{(B_{sx}-B_{mx})}{\sqrt{t(B_{sz}-B_{mz})+1}} \\ \frac{(B_{\mathrm{sy}}-B_{my})}{\sqrt{t(B_{sz}-B_{mz})+1}} \\ t^{\frac{1}{4}}\sqrt{t(B_{sz}-B_{mz})+1} \end{bmatrix} \tag{8}$$

where t, as shown at the bottom of the page.

According to equation (8), the number of equation unknowns is reduced from 6 to 3, and the coordinates $(x,\ y,\ z)$ of the capsule robot have the same coefficients and are only related to the longitudinal component m of the magnetic dipole moment [26]. When the specific coordinate origin is unknown, this paper adopts a relative positioning method to calculate the positioning error of the robot. The specific contents are as follows.

In the spatial coordinate system, take any point $W_1(x_1,\ y_1,\ z_1)$ as the datum point, and the coordinates of other points are $W_2(x_2,\ y_2,\ z_2)$, $W_3(x_3,\ y_3,\ z_3)\ldots W_n\ (x_n,\ y_n,\ z_n)$. The distance between W_1 and any point $W_i(1 < i < n+1)$ is l mm. The distances between the two points in the x-axis, y-axis and z-axis directions are $l_0,\ l_1,\ l_2$ (i.e., $l^2 = l_0^2 + l_1^2 + l_2^2$). The measured magnetic induction intensities of the two points are B_1 and B_i respectively. According to equation (8), equations (9) can be obtained:

$$\begin{bmatrix} \mathrm{x}_i \\ y_i \\ z_i \end{bmatrix} - \begin{bmatrix} x_1 \\ y_1 \\ z_1 \end{bmatrix} = \begin{bmatrix} l_0 \\ l_1 \\ l_2 \end{bmatrix}$$

$$\begin{bmatrix} \frac{x_i}{x_1} \\ \frac{y_i}{y_1} \\ \frac{z_i}{z_1} \end{bmatrix}$$

$$r^3 = |\mu| \times \{\frac{B_{\mathrm{s}z} - B_{mz} + \sqrt{9(B_{sz}-B_{mz})^2 + 8[(B_{sx}-B_{mx})^2 + (B_{sy}-B_{my})^2]}}{2[(B_{sz}-B_{mz})^2 + (B_{sx}-B_{mx})^2 + (B_{sy}-B_{my})^2]}\} \tag{7}$$

$$t = \frac{B_{sz} - B_{mz} + \sqrt{9(B_{sz}-B_{mz})^2 + 8[(B_{sx}-B_{mx})^2 + (B_{sy}-B_{my})^2]}}{2[(B_{sz}-B_{mz})^2 + (B_{sx}-B_{mx})^2 + (B_{sy}-B_{my})^2]}$$

$$= \begin{bmatrix} \dfrac{t_i^{\frac{4}{3}}(B_{sx_i}-B_{mx_i})}{t_1^{\frac{4}{3}}(B_{sx_1}-B_{mx_1})}\dfrac{\sqrt{t_1(B_{sz_1}-B_{mz_1})+1}}{\sqrt{t_i(B_{sz_i}-B_{mz_i})+1}} \\ \dfrac{t_i^{\frac{4}{3}}(B_{sy_i}-B_{my_i})}{t_1^{\frac{4}{3}}(B_{sy_1}-B_{my_1})}\dfrac{\sqrt{t_1(B_{sz_1}-B_{mz_1})+1}}{\sqrt{t_i(B_{sz_i}-B_{mz_i})+1}} \\ \dfrac{\sqrt{t_1(B_{sz_i}-B_{mz_i})+1}}{\sqrt{t_i(B_{sz_1}-B_{mz_1})+1}} \end{bmatrix} \tag{9}$$

If the coordinate W_i' (x_i', y_i', z_i') obtained from equation (9) and the distance between point a and reference point W_1 is l', the positioning error is shown in equation (10):

$$E_{beforecompensation} = |l' - l| \tag{10}$$

In the practical application of magnetic positioning, the motion of the capsule robot is affected by magnetic coupling, and the positioning accuracy decreases. Therefore, a compensation algorithm is needed to improve the positioning accuracy of the decoupled capsule robot. On the premise of many experiments, the method adopted in this paper is to fit the positioning error of each point obtained in equation (9) with the least square method. The actual position coordinates of the robot (relative to the selected datum point) are substituted into the fitting formula of the least square method in the three-axis direction. The fair value is used as the error compensation value of the calculation result of the positioning equation (8). The positioning errors of other points can also be obtained by this method. Thus, the magnetic positioning error compensation formula of the capsule robot can be obtained, as shown in equation (11):

$$\begin{bmatrix} x'' \\ y'' \\ z'' \end{bmatrix} = \frac{|10^{-7}m|^{\frac{1}{3}}t^{\frac{4}{3}}}{\sqrt{3}} \begin{bmatrix} \dfrac{(B_{sx}-B_{mx})}{\sqrt{t(B_{sz}-B_{mz})+1}} \\ \dfrac{(B_{sy}-B_{my})}{\sqrt{t(B_{sz}-B_{mz})+1}} \\ t^{\frac{1}{4}}\sqrt{t(B_{sz}-B_{mz})+1} \end{bmatrix} + \begin{bmatrix} x_{compensation} \\ y_{compensation} \\ z_{compensation} \end{bmatrix} \tag{11}$$

The coordinate of W_i' (x_i', y_i', z_i') after the algorithm compensation becomes $W_i''(x_i'+cmp, y_i'+cmp, z_i'+cmp)$, let the distance between the two points is l'', then the localization error of the robot after error compensation is shown in equation (12):

$$E_{aftercompensation} = |l'' - l| \tag{12}$$

The compensation algorithm adds a compensation amount based on the magnetic positioning algorithm. The subsequent positioning experiments show that the localization error $E_{aftercompensation}$ is much smaller than before compensation $E_{beforecompensation}$. Improve the magnetic positioning accuracy of the coupled capsule robot.

In summary, the specific steps of the magnetic localization algorithm proposed in this article are as follows:

(1) Pick a reference point;

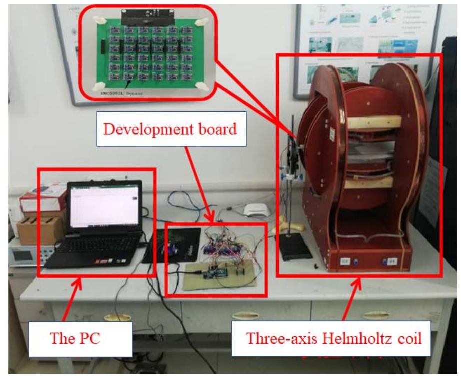

Fig. 3. Experimental platform.

(2) Measure the magnetic induction intensity of the selected localization coordinate points and reference points through the magnetic sensor array;

(3) Preliminarily calculate the localization error according to equation (8)-(9);

(4) Use the least square method to fit the error fitting curve of the selected coordinate points, and obtain the fitting equation;

(5) Substitute the actual coordinate point coordinates of the robot into the error compensation value of the fitting equation in step (4) to the magnetic localization algorithm;

(6) Substitute the error compensation value in step (5) into equation (8) to obtain the magnetic localization error compensation equation (12), and then use equation (12) to obtain the localization error of the robot after error compensation;

By comparing the errors in step (3) and step (6), it is verified by subsequent experiments that the positioning accuracy of the capsule robot is improved after error compensation.

III. Experimental Platform

The experimental platform is shown in Fig. 3, 6 × 6 Honeywell hmc5883 magnetic sensor array to measure the magnetic induction of capsule robot [27], [28]. The 36 magnetic sensors are connected through the built-in wires on the PCB and powered by the voltage module. The upper computer program is used to control the on-off of the relay and control each sensor's working state. The capsule robot is placed in a three-axis Helmholtz coil, and the external magnetic field of the capsule robot is controlled by changing the current of the input coil to measure the positioning of the capsule robot in different positions.

IV. Localization Experiments

A. Electromagnetics Simulation

The electromagnetic simulation software is used to establish a 1:1 three-dimensional model of the three-axis Helmholtz coil of the experimental platform. A permanent magnet is placed in the center of the magnetic field along the radial magnetization direction of the x-axis to provide a 1A current for the coaxial coil in the positive direction. By collecting the value of magnetic induction intensity, the capsule robot is positioned. The cloud diagram of magnetic induction intensity

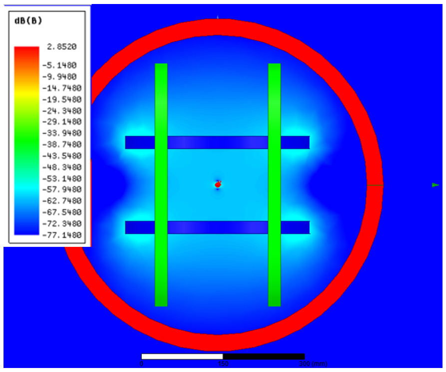

(a) Magnetic field nephogram of Helmholtz coil

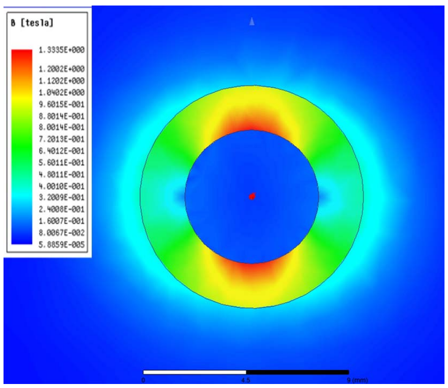

(b) Magnetic induction intensity of permanent magnet in capsule robot

Fig. 4. Magnetic induction nephogram.

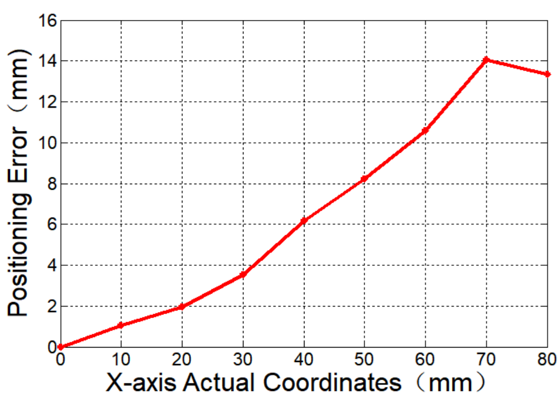

Fig. 5. x-axis localization error before compensation.

of permanent magnet in rotating magnetic field is shown in Fig. 4 [29].

B. Capsule Robot Localization Experiment Without Driving Magnetic Field

The robot is placed on the eight points respectively. The magnetic field strength of robot position is measured with step each 10mm. The y-axis and z-axis coordinates of the robot remains unchanged. The computer calculates the positioning error of the robot at each point through the corresponding algorithm equation. The error curve is shown in Fig. 5.

With the increase of the actual position distance of the capsule robot, the positioning error also increases, and the positioning accuracy is relatively low. In order to reduce the influence of external factors on the positioning accuracy of capsule robots, the least square method is proposed to fit the positioning error curve of capsule robots in three-dimensional space, as shown in Fig. 6. The red, blue, green, and black lines represent the original error curve and the least-squares method's first, second, and third fitting error curve. The equation of x-axis, y-axis and z-axis error fitting curve is shown in formula (13):

$$\begin{cases} E(x_1) = 0.1907x - 1.082 \\ E(x_2) = 0.0006x^2 + 0.1422x - 0.5163 \\ E(x_3) = -5 \times 10^{-5}x^3 + 0.0065x^2 - 0.04x + 0.32 \end{cases}$$
$$\begin{cases} E(y_1) = 0.1388y - 0.2164 \\ E(y_2) = 0.0003y^2 + 0.1131y - 0.49 \\ E(y_3) = 9.983 \times 10^{-5}y^3 - 0.0117y^2 + 0.47y - 1.2 \end{cases}$$
$$\begin{cases} E(z_1) = 0.1273z - 0.1 \\ E(z_2) = 0.0002z^2 + 0.1131z + 0.07 \\ E(z_3) = -2.6 \times 10^{-6}z^3 + 0.0005z^2 + 0.1z + 0.11 \end{cases} \tag{13}$$

In equation (13), (E (x_1), E (x_2), E (x_3)), (E (y_1), E (y_2), E (y_3)), (E (z_1), E (z_2), E (z_3)) represent the error curve equations after the first, second and third fitting of x-axis, y-axis and z-axis least-squares method respectively, and x, y and z represent the coordinate points initially selected by the capsule robot [30], [31].

C. Capsule Robot Localization Experiment With Driving Magnetic Field

When the capsule robot carries out the positioning experiment on the three-axis Helmholtz coil, it also needs to determine the coordinates of any two directions in space. In other directions, nine coordinate points of $0mm$, $10mm$, $20mm$, $30mm$, $40mm$, $50mm$, $60mm$, $70mm$, $80mm$ and $90mm$ are selected for error calculation. The error curve of capsule robot position coordinates before and after least square fitting is shown in Fig. 7. The red, blue, green, and black lines represent the original error curve and the least square method's first, second and third fitting error curve, respectively. It can be seen that after the algorithm compensation, the positioning accuracy of the capsule robot in the coil is improved. The error fitting curve equations of x-axis, y-axis and z-axis are shown in equation (14):

$$\begin{cases} E(x_1) = 0.1x - 1.78 \\ E(y_1) = 0.14y + 2.73 \\ E(z_1) = 0.17z - 1.66 \end{cases}$$
$$\begin{cases} E(x_2) = -0.0012x^2 + 0.206x + 0.7252 \\ E(y_2) = -0.0008y^2 + 0.19y + 1.462 \\ E(z_2) = 0.001z^2 + 0.06z + 0.4388 \end{cases}$$
$$\begin{cases} E(x_3) = 10^{-6}x^3 - 0.01x^2 + 0.6x - 0.85 \\ E(y_3) = 4.41 \times 10^{-5}y^3 - 0.07y^2 + 0.4y + 0.35 \\ E(z_3) = -1.4 \times 10^{-5}z^3 + 0.003z^2 - 0.01z + 0.8 \end{cases} \tag{14}$$

In order to better simulate the human intestinal environment, several groups of path experiments were designed in the

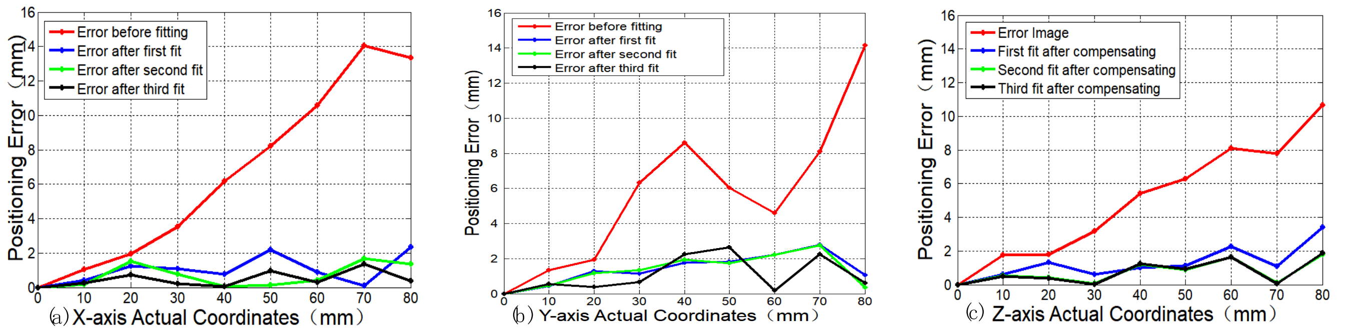

Fig. 6. (a) Comparison curve of localization error before and after x-axis least square fitting; (b) Comparison curve of localization error before and after y-axis least square fitting; (c) Comparison curve of localization error before and after z-axis least square fitting.

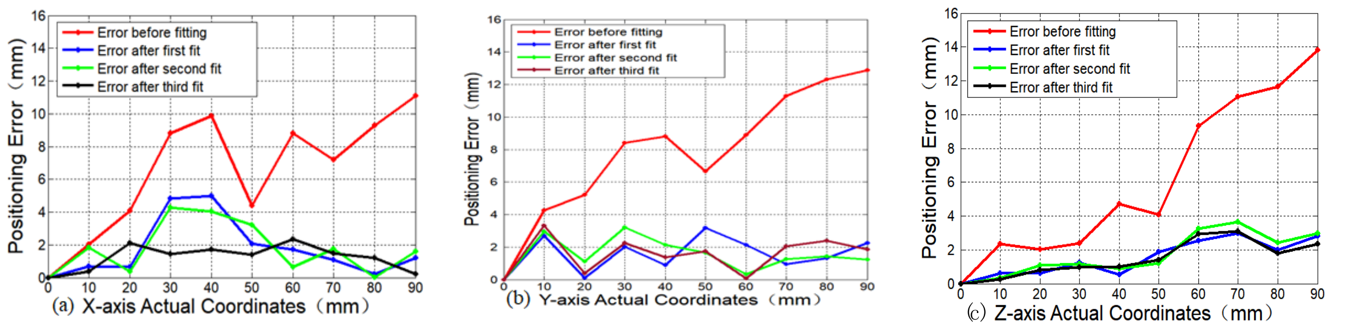

Fig. 7. (a) Comparison curve of localization error before and after x-axis least square fitting; (b) Comparison curve of localization error before and after y-axis least square fitting; (c) Comparison curve of localization error before and after z-axis least square fitting.

three-axis Helmholtz coil. The first group of path experiments is to simulate the broken line path. Firstly, we keep the x-axis coordinate of the capsule robot unchanged and place the robot in the coil along the z-axis, 150 mm away from the sensor. When the robot moves along the y-z plane, the positioning image of the capsule robot before and after compensation by the algorithm is shown in Fig. 8.

The red and blue curves in Fig. 8 represent the desired position of the capsule robot and the position compensated by the algorithm after measurement, respectively. Through comparison, we can see that the positioning effect of the capsule robot is better after algorithm compensation. The specific positioning parameters of the path are shown in Table I.

According to Table I, the localization accuracy of the compensated capsule robot is 2.29*mm*, which means that the localization accuracy of the algorithm is relatively good.

When the trajectory of the capsule robot is square, the localization image is shown in Fig. 9.

In Fig. 9, the red curve represents the desired position of the capsule robot, and the blue curve represents the position of the capsule robot after algorithm compensation. The positioning parameters are shown in Table II.

According to the calculation in Table II, the localization accuracy of the capsule robot after compensation is 1.80*mm*.

TABLE I

POSITION PARAMETERS OF BROKEN LINE PATH INSIDE COIL $\left(l = \sqrt{\begin{array}{c}(X_{beforecmp} - X_{aftecmpr})^2 + (Y_{beforecmp} - Y_{aftercmp})^2 \\ +(Z_{beforecmp} - Z_{aftecmp})^2\end{array}}\right)$

Desired value (*mm*)	Measured value (*mm*)	Error (*mm*)	Error distance (*mm*)
(0.00,0.00)	(0.00,0.00)	(0.00,0.00)	0.00
(5,5)	(6.75,5.99)	(1.75,0.99)	2.01
(10,25)	(10.87,25.84)	(0.87,0.84)	1.21
(22.5,30)	(24.95,30.80)	(2.45,0.80)	2.58
(35,35)	(37.63,36.61)	(2.63,1.61)	3.08
(47.5,30)	(49.06,32.41)	(1.56,2.41)	2.87
(60,25)	(63.07,25.31)	(3.07,0.31)	3.09
(65,12.5)	(65.57,14.38)	(0.57,1.88)	1.96
(70,0)	(71.95,3.25)	(1.95,3.25)	3.79

D. The Influence of Magnetic Coupling on Localization Accuracy

In order to verify the accuracy of the compensation algorithm, a set of comparative experiments are carried out in the driving magnetic field (with magnetic coupling). Taking the circular motion path of the robot as an example, the path positioning curves of the capsule robot with and without magnetic coupling compensation are made, respectively. As shown in Fig. 10, the red curve represents the actual position of the capsule robot, and the blue curve represents the positioning curve of the capsule robot without magnetic coupling compensation. The average positioning error is 5.64*mm*; the black curve represents the positioning curve of the capsule robot with magnetic coupling compensation, and the average positioning error is 2.62*mm*. Therefore, after compensating for the positioning error, the positioning accuracy is improved by 53.5%.

TABLE II
POSITION PARAMETERS OF BROKEN LINE PATH INSIDE COIL

$$\left(l = \sqrt{\begin{array}{c}(X_{beforecmp} - X_{aftecmpr})^2 + (Y_{beforecmp} - Y_{aftercmp})^2 \\ +(Z_{beforecmp} - Z_{aftecmp})^2\end{array}}\right)$$

Desired value (mm)	Measured value (mm)	Error (mm)	Error distance (mm)
(15,15)	(12.57,12.50)	(2.43,2.50)	3.49
(15,25)	(13.36,24.77)	(1.64,0.23)	1.66
(15,35)	(14.61,34.68)	(0.39,0.32)	0.50
(15,45)	(14.38,43.41)	(0.62,1.59)	1.71
(15,55)	(13.52,52.93)	(1.48,2.07)	2.54
(15,65)	(12.80,62.97)	(2.20,2.03)	2.99
(25,65)	(23.19,64.14)	(1.81,0.86)	2.00
(35,65)	(34.56,64.44)	(0.44,0.56)	0.71
(45,65)	(44.37,64.81)	(0.63,0.19)	0.66
(55,65)	(54.53,64.06)	(0.47,0.94)	1.05
(65,65)	(63.75,64.01)	(1.25,0.99)	1.59
(65,55)	(64.95,52.32)	(0.05,2.68)	2.68
(65,45)	(63.37,43.61)	(1.63,1.39)	2.14
(65,35)	(63.31,32.17)	(1.69,2.83)	3.30
(65,25)	(63.94,24.91)	(1.06,0.09)	1.06
(65,15)	(63.67,14.29)	(1.33,0.71)	1.51
(55,15)	(54.68,13.13)	(0.32,1.87)	1.90
(45,15)	(45.00,14.19)	(0.00,0.81)	0.81
(35,15)	(34.65,13.16)	(0.35,1.84)	1.87
(25,15)	(23.37,14.42)	(1.63,0.58)	1.73
(15,15)	(12.57,12.50)	(2.43,2.50)	3.49

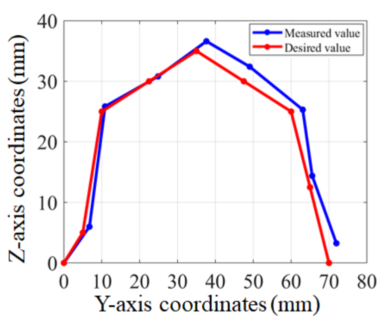

Fig. 8. Localization curve of broken line path in coil.

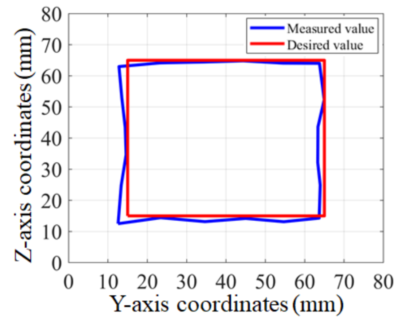

Fig. 9. Localization curve of square line path in coil.

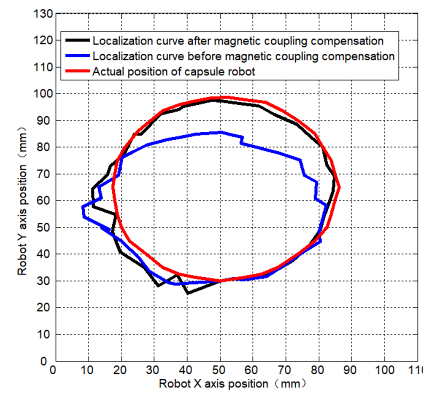

Fig. 10. Comparison image of capsule robot localization curve with or without magnetic coupling compensation.

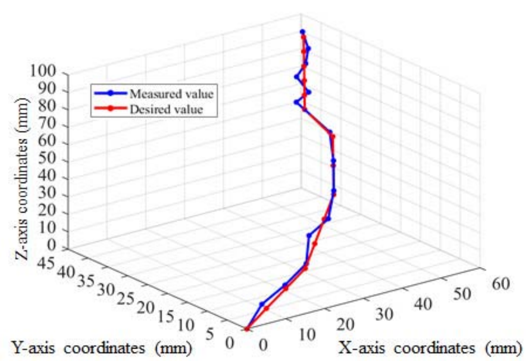

Fig. 11. Three-dimensional planning path localization curve.

E. Localization Experiment of Arbitrary Curve in Space

It can be seen from Table I and Table II that the positioning accuracy of the capsule robot is significantly improved after using the compensation algorithm. Therefore, the algorithm compensation experiment in three-dimensional space is carried out to verify the algorithm's accuracy further. The planning path is selected as an arc, and the positioning image of the path is shown in Fig. 11.

The red and blue curves in Fig. 11 represent the desired position of the capsule robot and the position after using the compensation algorithm, respectively. Through comparison, it is found that there is little difference between the two curves. The results show that the positioning accuracy of the capsule robot is 1.79mm. The positioning error of the algorithm in three-dimensional space is small, and the positioning effect is good. Therefore, the algorithm is still suitable for the positioning of the capsule robot in three-dimensional space.

F. Comparison With Other Localization Methods

In order to verify the effectiveness of the magnetic positioning algorithm proposed in this article, this chapter carefully compares the localization accuracy of capsule robots studied by other scientific research teams. The specific results are shown in Table III.

It can be seen from Table III that the positioning accuracy of the magnetic positioning algorithm studied by other experimental teams is more than 4mm. The average positioning accuracy of the magnetic positioning algorithm proposed in

TABLE III
POSITIONING ACCURACY COMPARISON TABLE

Research team	Range of motion	Experiment platform	Localization accuracy
Shanghai Jiao Tong University [4]	3-D	Hall sensor array	8*mm*
South China University of Technology [29]	3-D	Wearable sensor array platform	10.7*mm*
Harbin Institute of Technology [8]	3-D	Wearable sensor array platform	4.9*mm*
Chongqing University [12]	2-D	PNI magnetic flux sensor array	9.53*mm*
Tianjin University of Technology	3-D	Three-axis Helmholtz coil	2.25*mm*
Kagawa University [30]	2-D	Hall sensor array	6.09*mm*

this paper is 2.25mm, which is high. Compared with other teams' positioning experiments on two-dimensional plane, this paper's positioning technology has risen to three-dimensional space. Furthermore, the three-axis Helmholtz coil drives experiments, eliminating the external interference of magnetic coupling on the positioning. Therefore, the magnetic localization algorithm in this paper has a better practical effect.

V. CONCLUSION

Aiming at the magnetic coupling problem between the magnetic field generated by the capsule robot embedded with a permanent magnet and the magnetic field generated by the three-axis Helmholtz coil in the magnetic positioning system, a magnetic positioning algorithm is proposed to solve the magnetic coupling problem between the driving magnetic field and the permanent magnet in the capsule robot. According to the magnetic dipole model, a series of formulas reduces the number of unknowns from 6 to 3. Based on the magnetic positioning algorithm, a compensation amount is added to the compensation algorithm. The experimental results show that the positioning accuracy of the capsule robot is improved after decoupling. The simulation results show that the positioning accuracy of the calculated path is 2.62*mm*. Three paths are used to simulate the internal environment of the human gastrointestinal tract, and the positioning accuracy is 1.80*mm*, 3.06*mm* and 1.79*mm*, respectively. The accuracy of the proposed magnetic positioning compensation algorithm is verified. The positioning accuracy of the algorithm in practical application is also disturbed by other external factors, such as human body shaking, which is also our next research direction.

REFERENCES

[1] L. Q. Dong, "Review, current status and progress of gastrointestinal endoscopy and imaging methods," *J. Clin. Radiol.*, vol. 8, no. 8, pp. 662–666, Aug. 2002.
[2] J. Suo *et al.*, "Diagnosis and treatment of early gastric cancer," *Chin. J. Pract. Surg.*, vol. 31, no. 8, pp. 717–719, Aug. 2011.
[3] S. T. Qi *et al.*, "Surgical robot system and its clinical application," *Chin. Med. Equip.*, vol. 26, no. 6, pp. 56–59, Jun. 2011.
[4] P. P. Jiang *et al.*, "A method for *in vitro* continuous tracking and location of human whole digestive tract physiological parameters telemetry capsules," *J. Shanghai Jiao Tong Univ.*, vol. 39, no. 5, pp. 864–868, Jun. 2005.
[5] P. P. Jiang *et al.*, "Electromagnetic tracking and positioning method for *in vivo* capsule telemetry system," *Opt. Precis. Eng.*, vol. 15, no. 8, pp. 1247–1252, Aug. 2007.
[6] D. Kun *et al.*, "Electronic capsules positioning system based on permanent magnetic field," *J. Biomed. Eng.*, vol. 22, no. 2, pp. 123–136, Oct. 2008.
[7] K. Ma *et al.*, "Design of positioning and tracking system based on electromagnetic induction principle," *Packag. Eng.*, vol. 38, no. 11, pp. 153–158, Oct. 2017.
[8] L. Yang *et al.*, "Target tracking and positioning technology based on magnetic sensor array," M.S. thesis, Harbin Inst. Technol., Harbin, China, 2010.
[9] S. Song, C. Hu, and M. Q.-H. Meng, "Multiple objects positioning and identification method based on magnetic localization system," *IEEE Trans. Magn.*, vol. 52, no. 10, pp. 1–7, Oct. 2016.
[10] F. Carpi, N. Kastelein, M. Talcott, and C. Pappone, "Magnetically controllable gastrointestinal steering of video capsules," *IEEE Trans. Biomed. Eng.*, vol. 58, no. 2, pp. 231–234, Feb. 2011.
[11] K. Shiba, T. Nagato, T. Tsuji, and K. Koshiji, "Analysis of specific absorption rate and current density in an energy transmission system for a wireless capsule endoscope," in *Proc. 29th Annu. Int. Conf. IEEE Eng. Med. Biol. Soc.*, Aug. 2007, pp. 6051–6054.
[12] D. Li, F. Niu, J. Li, X. Li, and D. Sun, "Gradient-enhanced electromagnetic actuation system with a new core shape design for microrobot manipulation," *IEEE Trans. Ind. Electron.*, vol. 67, no. 6, pp. 4700–4710, Jun. 2020.
[13] S. X. Yang, A. Zhu, G. Yuan, and M. Q.-H. Meng, "A bioinspired neurodynamics-based approach to tracking control of mobile robots," *IEEE Trans. Ind. Electron.*, vol. 59, no. 8, pp. 3211–3220, Aug. 2012.
[14] P. Ryan and E. Diller, "Magnetic actuation for full dexterity microrobotic control using rotating permanent magnets," *IEEE Trans. Robot.*, vol. 33, no. 6, pp. 1398–1409, Dec. 2017.
[15] Y. Liao, "*In vitro* magnetic tracking and positioning system based on Hall sensor array," *Beijing Biomed. Eng.*, vol. 31, no. 5, pp. 501–506, Oct. 2012.
[16] Y. P. Ren, "A compensation method for interference of human body movement to magnetic positioning of capsule endoscope," *Chin. J. Sensor Technol.*, vol. 28, no. 11, pp. 1640–1646, Nov. 2015.
[17] M. Wang, Q. Shi, S. Song, C. Hu, and M. Q.-H. Meng, "A novel relative position estimation method for capsule robot moving in gastrointestinal tract," *Sensors*, vol. 19, no. 12, pp. 2746–2763, 2019.
[18] Y. P. Ren, "An accurate positioning technique of wireless capsule endoscope based on magnetic sensor array," M.S. thesis, Tianjin Univ., Taiyuan, China, 2016.
[19] S. D. Niu, "Capsule endoscopic positioning technology based on magnetic sensing," M.S. thesis, Taiyuan Univ., Taiyuan, China, 2017.
[20] Q. Fu, S. Guo, Y. Yamauchi, H. Hirata, and H. Ishihara, "A novel hybrid microrobot using rotational magnetic field for medical applications," *Biomed. Microdevices*, vol. 17, no. 2, pp. 1–12, Feb. 2015.
[21] Q. Fu, S. Guo, S. Zhang, H. Hirata, and H. Ishihara, "Characteristic evaluation of a shrouded propeller mechanism for a magnetic actuated microrobot," *Micromachines*, vol. 6, no. 9, pp. 1272–1288, Sep. 2015.
[22] Q. Fu, S. Zhang, S. Guo, and J. Guo, "Performance evaluation of a magnetically actuated capsule microrobotic system for medical applications," *Micromachines*, vol. 17, no. 2, pp. 1–12, Oct. 2018.
[23] Q. Fu, S. Guo, Q. Huang, H. Hirata, and H. Ishihara, "Development and evaluation of novel magnetic actuated microrobot with spiral motion using electromagnetic actuation system," *J. Med. Biol. Eng.*, vol. 36, no. 4, pp. 506–514, Jul. 2016.
[24] Z. C. Cai *et al.*, "Performance evaluation of a magnetically driven microrobot for targeted drug delivery," *Micromachines*, vol. 12, no. 10, p. 1210, Oct. 2021.
[25] H. Li, "Research on space voltage vector control model of universal rotating magnetic field," M.S. thesis, Dalian Univ. Technol., Dalian, China, 2019.

[26] Z. Cai *et al.*, “Performance evaluation of a magnetically driven microrobot for targeted drug delivery,” *Micromachines*, vol. 12, no. 10, p. 1210, 2021.
[27] Y. N. Wang, “A sufficient condition for least squares estimator to be better than instrumental variable estimator,” *J. Wenzhou Univ., Natural Sci. Ed.*, vol. 42, no. 1, pp. 1–5, Feb. 2021.
[28] J. D. Xu, “OTSU fast image segmentation method based on least square fitting,” *J. Changzhou Univ., Natural Sci. Ed.*, vol. 33, no. 1, pp. 70–76, Jan. 2021.
[29] J. L. Wang and L. B. Hu, “Research on the magnetic field of Helmholtz coil,” *Think Tank Times*, vol. 44, no. 44, pp. 278–279, Nov. 2019.
[30] H. Li *et al.*, “Analysis of magnetic field uniformity of triaxial orthogonal Helmholtz coil,” *Mod. Mach.*, vol. 48, no. 4, pp. 1–5, Oct. 2019.
[31] T. Okada, S. Guo, N. Xiao, F. Qiang, and Y. Yamauchi, “Control of the wireless microrobot with multi-DOFs locomotion for medical applications,” in *Proc. IEEE Int. Conf. Mechatronics Autom.*, Chengdu, China, Aug. 2012, pp. 2405–2410.

Qiang Fu received the Ph.D. degree in intelligent mechanical systems engineering from Kagawa University, Japan, in 2017. He is currently an Associate Professor with Tianjin University of Technology, Tianjin, China. His current research interest includes biomedical robots, such as the development of multi-module magnetic actuated microrobotic systems for biomedical applications.

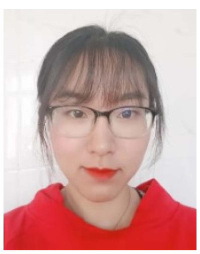

Chunliu Fan is currently pursuing the M.S. degree with the College of Electrical and Electronic Engineering, Tianjin University of Technology, Tianjin, China. His research interests include the magnetic driven capsule robot, bionic fish microrobots, and control method of self-reconfigurable microrobot.

Xinrui Wang received the M.S. degree in electrical and electronic engineering from the Tianjin University of Technology in 2021. His main research interests include control methods for micro-robots and magnetic positioning algorithms for magnetically driven capsule robots.

Songyuan Zhang received the Ph.D. degree in intelligent mechanical systems engineering from Kagawa University, Japan, in 2016. He is currently an Associate Professor with the State Key Laboratory of Robotics and System, Harbin Institute of Technology, China. His research interests include bio-inspired robotics, human–robot interaction, and medical robots.

Xi Zhang is currently pursuing the M.S. degree with the College of Electrical and Electronic Engineering, Tianjin University of Technology, Tianjin, China. His research interests include the design and control method of the microrobot, and control method of self-reconfigurable microrobot.

Jian Guo received the Ph.D. degree in intelligent mechanical systems engineering from Kagawa University, Japan, in 2012. He is currently a Full Professor with Tianjin University of Technology, Tianjin, China. His current research interest includes biomedical robots, such as wireless microrobots in pipe and robotic catheter systems for biomedical applications.

Shuxiang Guo (Fellow, IEEE) received the Ph.D. degree in mechanoinformatics and systems from Nagoya University, Japan, in 1995. He is currently a Full Professor with the Faculty of Engineering and Design, Kagawa University, Japan. He received the Chang Jiang Professorship Award from the Ministry of Education of China in 2005. He is the Editor-in-Chief of the *International Journal of Mechatronics and Automation*.